High-NOON States by Mixing Quantum and Classical Light

Itai Afek, Oron Ambar, Yaron Silberberg*

Precision measurements can be brought to their ultimate limit by harnessing the principles of quantum mechanics. In optics, multiphoton entangled states, known as NOON states, can be used to obtain high-precision phase measurements, becoming more and more advantageous as the number of photons grows. We generated "high-NOON" states ($N = 5$) by multiphoton interference of quantum down-converted light with a classical coherent state in an approach that is inherently scalable. Super-resolving phase measurements with up to five entangled photons were produced with a visibility higher than that obtainable using classical light only.

Entanglement is a distinctive feature of quantum mechanics that lies at the core of many new applications in the emerging science of quantum information. Multiparticle entangled states are central to quantum computing, quantum teleportation, and quantum metrology (*1*). A particularly useful class of states are the maximally path-entangled multiphoton entangled states (NOON states)

$$|N{::}0\rangle_{A,B} \equiv \frac{1}{\sqrt{2}}\left(|N,0\rangle_{A,B} + |0,N\rangle_{A,B}\right) \quad (1)$$

Department of Physics of Complex Systems, Weizmann Institute of Science, Rehovot 76100, Israel.

*To whom correspondence should be addressed. E-mail: yaron.silberberg@weizmann.ac.il

which contain N indistinguishable particles in an equal superposition of all being in one of two possible paths A and B (*2*). These states are "Schrödinger cats," as they consist of a superposition of two highly distinct states corresponding to the "dead and alive" cat. The larger the value of N, the bigger the cat is, thus bringing us closer to the regime of macroscopic entanglement envisioned originally by Schrödinger (*3*). Realization of such states is required for the experimental study of fundamental questions such as the effect of decoherence on many-particle entanglement (*4*, *5*). In addition, NOON states are the enabling technology behind various quantum measurement schemes. In optics, a NOON state with N entangled photons acquires a phase at a rate N times as fast as classical light (*6*). This leads to enhanced phase sensitivity, which can be used for reaching the fundamental Heisenberg limit (*2*), and to phase super-resolution, which is the key to sub-Rayleigh resolution in quantum lithography (*7*). NOON states based on nuclear spin (*8*) and atomic spin waves (*9*) have also been shown to allow enhanced measurement sensitivity.

Our goal is to generate optical NOON states with high photon numbers. Various schemes for generating such states have been suggested (*2*, *10*–*15*). However, existing realizations (*16*–*18*) have been limited to three-photon states. We note that a "NOON-like" four-photon state has been generated, but only by using four rather than two spatial modes (*19*). In addition, a number of experiments have used state projection to focus on the NOON component of various initial N-photon states (*20*–*23*).

We present an experimental realization of an approach that yields NOON states with arbitrarily high photon numbers (*24*, *25*). The underlying principle is that when a classical coherent state and quantum down-converted light are mixed properly using a standard beamsplitter, the emerging state shows "Schrödinger cat"–like behavior; that is, virtually all the photons exit collectively from one of the beamsplitter ports or the other (Fig. 1A). The approach is appealing because of its inherent simplicity, as it relies on a fundamental unmodified multiphoton interference effect. Consider a 50/50 beamsplit-

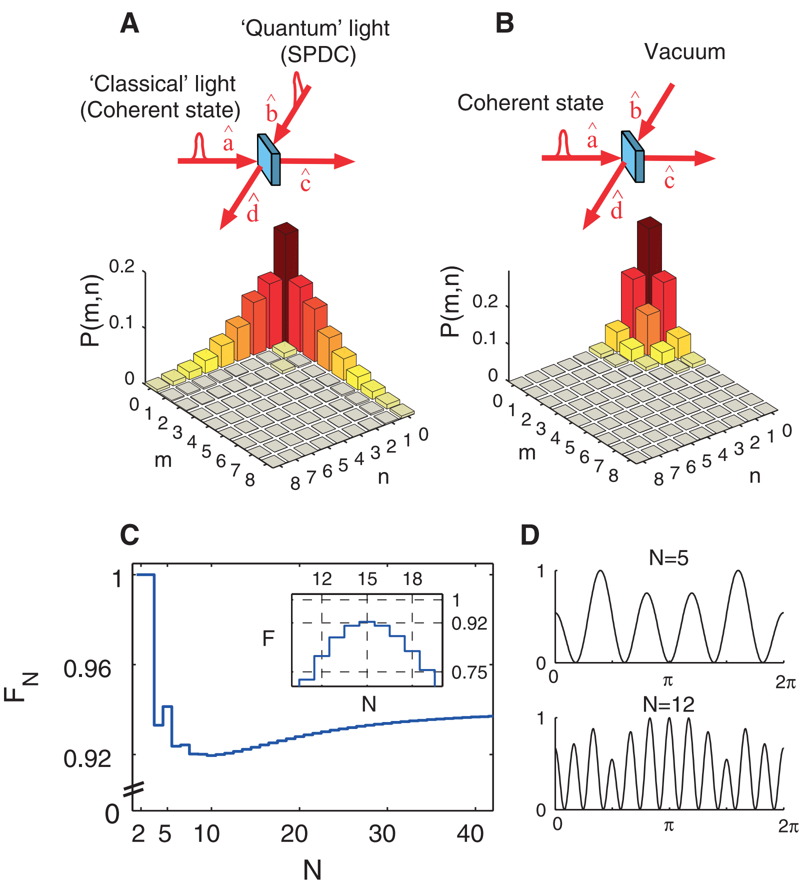

Fig. 1. Theoretical properties of the generated states. (**A**) Classical light is mixed on a beamsplitter with quantum photon pairs produced by collinear SPDC. Bar heights represent the probability for m, n photons in output modes c, d, respectively. The "corner"-like shape illustrates the tendency of all the photons to collectively exit from the same output port, exhibiting "Schrödinger cat"–like behavior. The effect occurs for arbitrary photon fluxes and is demonstrated here using 1.2 photons per pulse from each input. (**B**) The same as (A) but using only the classical light, shown for comparison. The photons at the outputs are clearly in a separable (unentangled) state. (**C**) Fidelity F_N versus N in an ideal setup. The pair amplitude ratio γ, which maximizes the NOON state overlap, was chosen separately for each N. Optimal fidelity is always larger than 0.92, and it approaches 0.943 asymptotically for large N. The inset shows that when γ is optimized for $N = 15$, the fidelity for nearby N is also high. In this case $F > 0.75$ for $N = 12$ to 19, simultaneously. (**D**) Simulated N-fold coincidences as a function of Mach-Zehnder phase for $N = 5$ or 12, demonstrating N-fold super-resolution.

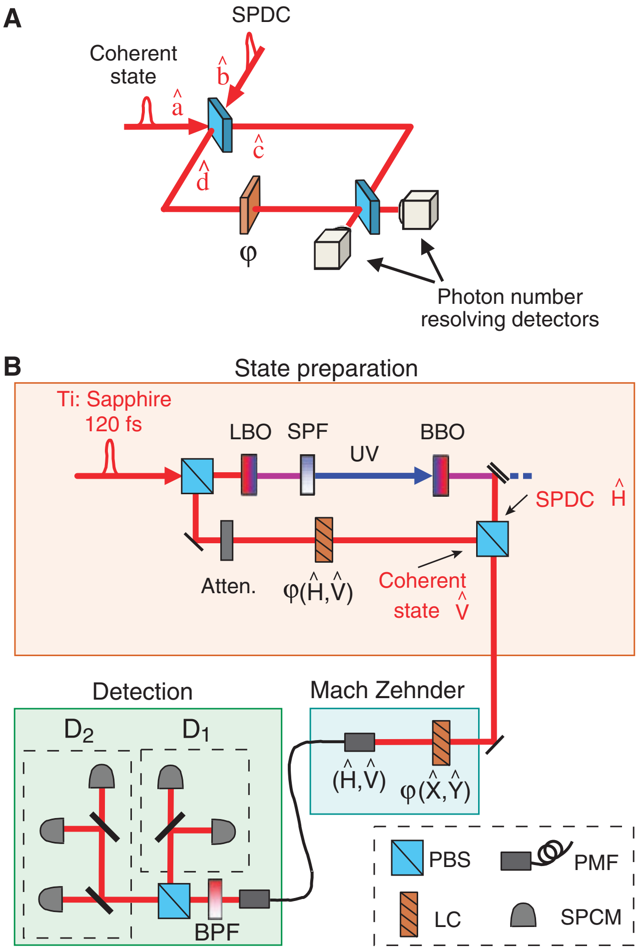

Fig. 2. Experimental setup. (**A**) Schematic of the setup depicting a Mach-Zehnder interferometer (MZ) fed by a coherent state and SPDC. The NOON states occur in modes $\hat{c}$ and $\hat{d}$ after the first beamsplitter. Measurement of multiphoton coincidences is performed using photon number–resolving detectors. (**B**) Detailed layout of the setup. A pulsed Ti:sapphire oscillator with 120-fs pulses at a repetition rate of 80 MHz is doubled using a 2.74-mm lithium triborate (LBO) crystal to obtain 404-nm ultraviolet pulses with maximum power of 225 mW. These pulses then pump collinear degenerate type I SPDC at 808 nm using a 1.78-mm beta barium borate (BBO) crystal. The SPDC ($\hat{H}$ polarization) is mixed with attenuated coherent light ($\hat{V}$ polarization) using a polarizing beamsplitter (PBS). A thermally induced drift in the relative phase is corrected every few minutes with the use of a liquid crystal (LC) phase retarder. The MZ is polarization-based in a collinear, inherently phase-stable design. The MZ phase is controlled using an additional LC phase retarder at 45°, which adjusts the phase between $\hat{X}$ and $\hat{Y}$ polarizations. The spatial and spectral modes are matched using a polarization-maintaining fiber (PMF) and a 3-nm (full width at half maximum) bandpass filter (BPF). Photon number–resolving detection is performed using an array of single-photon counting modules (SPCM, Perkin Elmer).

ter fed by a coherent state, $|\alpha\rangle_a$, in one input port and collinear degenerate spontaneous parametric down-conversion (SPDC), $|\xi\rangle_b$, in the other (Fig. 1A). The input states are defined in the conventional way (*6*):

$$|\alpha\rangle = \sum_{n=0}^{\infty} \exp\left(-\frac{1}{2}|\alpha|^2\right)\frac{\alpha^n}{\sqrt{n!}}|n\rangle,$$
$$\alpha = |\alpha|\ \exp(i\theta_{cs}) \qquad (2)$$

$$|\xi\rangle = \frac{1}{\sqrt{\cosh r}}\sum_{m=0}^{\infty}(-1)^m\frac{\sqrt{(2m)!}}{2^m m!}(\tanh r)^m|2m\rangle \qquad (3)$$

where the phase of $|\xi\rangle$ has been set arbitrarily to zero, leaving the relative phase of the two inputs to be determined by θ_{cs}. We denote the pair amplitude ratio of the coherent state and SPDC inputs by $\gamma \equiv |\alpha|^2/r$. In physical terms, γ^2 is the two-photon probability of the classical source divided by that of the quantum source. The larger the value of γ, the higher the relative weight of the classical resources. The state at the beamsplitter output, $|\psi_{out}\rangle_{c,d}$, is highly path-entangled. A general N-photon two-mode state can be written as $\sum_{k=0}^{N}u_k|k\rangle_c|N-k\rangle_d$. The creation of an ideal NOON state would require elimination of all the "non-NOON" components (i.e., $u_1, \ldots, u_{N-1} = 0$). The present scheme does this almost perfectly by using the naturally emerging multiphoton interference (Fig. 1A). The fidelity of the output state's normalized N-photon component, $|\psi^N_{out}\rangle$, with a NOON state is $F_N \equiv |\langle N{::}0|\psi^N_{out}\rangle|^2$. It can be shown that by choosing $\theta_{cs} = \pi/2$ and optimizing γ for each N, one can achieve $F_N > 0.92$

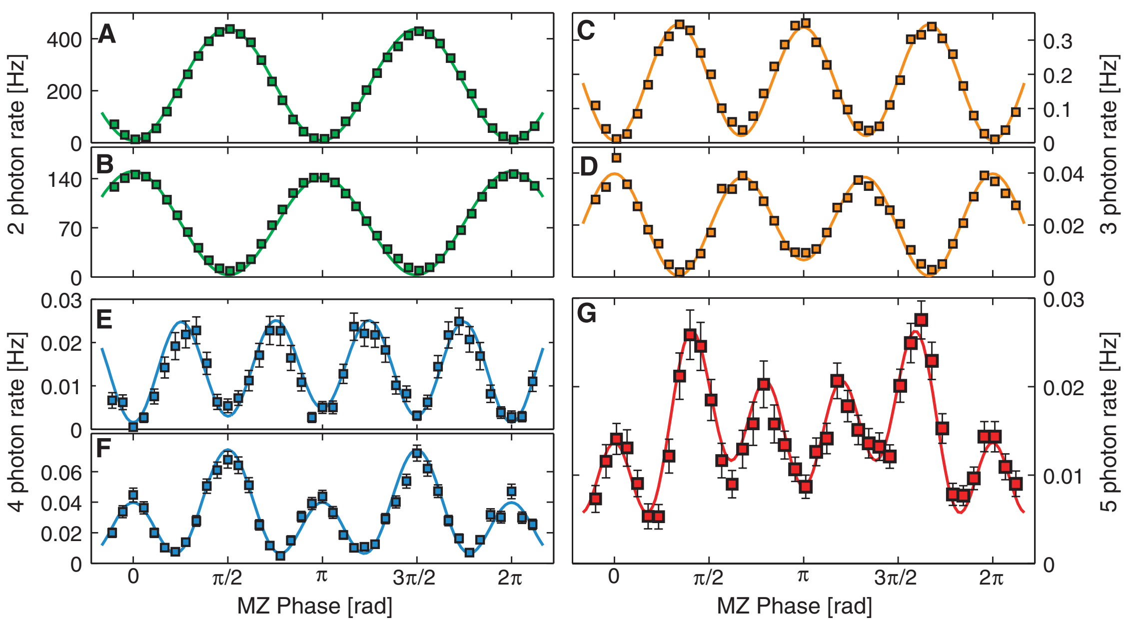

Fig. 3. Experimental results: Coincidence measurements demonstrating N-fold super-resolution for N = 2, 3, 4, and 5 with no background subtraction. Error bars indicate ±σ statistical uncertainty. Solid lines are obtained using an analytical model (*26*). Numbers of simultaneous "clicks" in detectors D_1 and D_2 are denoted N_1 and N_2, respectively (Fig. 2B). (**A** and **B**) Two-photon rate with N_1, N_2 = 1, 1 (A) and N_1, N_2 = 2, 0 (B). (**C** and **D**) Three-photon rate with N_1, N_2 = 2, 1 (C) and N_1, N_2 = 3, 0 (D). (**E** and **F**) Four-photon rate with N_1, N_2 = 3, 1 (E) and N_1, N_2 = 2, 2 (F). (**G**) Five-photon rate with N_1, N_2 = 3, 2. For each N the pair amplitude ratio γ was chosen separately to maximize the NOON state fidelity. The optimal values (obtained analytically) are $\gamma_2 = \gamma_3 = 1$, $\gamma_4 = \sqrt{3}$, and $\gamma_5 = 9/(\sqrt{10}+1) \approx 2.16$. Visibility of the sinusoidal patterns with N oscillations is determined by a weighted least-squares sine-cosine decomposition restricted to frequencies of 0, 1, …, N (*27*). The values for plots (A) to (G) are V = 95 ± 0.0%, 88 ± 0.03%, 86 ± 0.6%, 80 ± 1.9%, 74 ± 3%, 73 ± 2.4%, and 42 ± 2%, respectively.

for arbitrary N (Fig. 1C). The theoretical overlaps for the states generated in this work are $F_N = 1$, 1, 0.933, and 0.941 for $N = 2$, 3, 4, and 5, respectively. We note that the four-photon value is much higher than the theoretical fidelity of 0.75 obtainable using down-conversion only (*22*, *23*).

To verify the N-photon coherence of the generated states, we use a Mach-Zehnder interferometer (Fig. 2). This is the prototypical setup used in schemes for quantum lithography and reduced-noise interferometry (*2*). The quantum and classical inputs are prepared in perpendicular linear polarizations (H, V) and spatially overlapped using a polarizing beamsplitter. A Mach-Zehnder interferometer (MZ) is then implemented in an inherently phase-stable, collinear design so that the NOON state mode subscripts c, d may now be replaced by X, Y (±45° polarizations). After application of the MZ phase shift φ, the state $|N, 0\rangle_{X,Y} + |0, N\rangle_{X,Y}$ evolves to $|N, 0\rangle_{X,Y} + \exp(iN\varphi)|0, N\rangle_{X,Y}$. This gives rise to interference oscillations N times as fast as those of a single photon with the same frequency (*2*).

In the experimental results (Fig. 3), two- to five-photon coincidence rates were measured as a function of the MZ phase. We denote the number of photon "clicks" in detectors D_1 and D_2 as N_1 and N_2, respectively. The N_1, N_2 coincidence rate is expected to demonstrate a de Broglie wavelength (*6*) of λ/N, where $N = N_1 + N_2$ is the total number of photons. The red curves are produced by an analytical model of the experiment, accounting for the overall transmission and the positive operator-value measures of the detectors (*26*). The two- and three-photon results were measured simultaneously with $\gamma_2 = \gamma_3 = 1$ (the subscript of γ denotes the value of N for which it was optimized) using a mere 2 mW of ultraviolet power to pump the SPDC. The results in Fig. 3, C and D, show a visibility of 86 ± 0.6% for 2, 1 photons and 80 ± 1.9% for 3, 0 photons. The four-photon measurements were taken with $\gamma_4 = \sqrt{3}$ and 25 mW of ultraviolet pump power. They exhibit similar visibilities for the 3, 1 and the 2, 2 options: 74 ± 3% and 73 ± 2.4%, respectively (Fig. 3, E and F). Finally, the $N = 5$ NOON state has a visibility of $V = 42 \pm 2\%$ for 3, 2 photons and was taken using 215 mW of ultraviolet pump power and setting $\gamma_5 = 9/(\sqrt{10} + 1) \approx 2.16$ (Fig. 3G), implying that $\gamma_5^2 \approx 4.7$ times as many photon pairs originate from the coherent state as from the SPDC. All the above visibilities manifest the high NOON-state overlap of the generated states. These visibilities significantly exceed the super-resolution bound for classical states, which we have recently derived (*27*). In particular, the classical bound for the five-photon measurement is 16.67%, which is surpassed here by more than 12 standard deviations. The visibility of the experimental plots is determined by the overall setup transmission, which we denote as η. For $\eta < 1$, high-order events contribute a background to the N-fold coincidence rate. In the current setup we estimate $\eta \approx 0.12$ on the basis of the SPDC coincidence-to-singles ratio.

The realized scheme works naturally for arbitrary N (*24*). This requires no alterations to the setup, except for the use of detectors that can resolve N-photon events and setting γ appropriately. This is in contrast to previous experiments that were customized to a specific value of N (*16*–*18*). Our implementation is limited to $N = 5$ mainly by the overall setup transmission ($\eta \approx 0.12$). A higher value would allow the generation of even larger states (*26*). Furthermore, most of the photons in this scheme originate from the coherent (classical) light source, which is practically unlimited in intensity. This eliminates the need for bright SPDC sources, providing experimental simplification. Finally, the scheme involves no state projection or post-selection, implying that all the N-photon events contribute to the measurable N-photon interferences.

The N-fold coincidence plots of Fig. 1D exhibit N zero points, as expected from perfect maximally path-entangled states, albeit with somewhat modulated peak heights. In fact, it has been shown (*24*) that as a result of the high fidelity, we can expect a phase sensitivity that is only slightly lower than the Heisenberg limit for a given N-photon component. Thus, the small deviation from an ideal NOON state is not a major limiting factor and is more than compensated for by the intrinsic 100% efficiency. Furthermore, although the state at hand is optimized for a given $N = N_0$, there is a range of N values surrounding N_0 that also have considerable NOON fidelity (Fig. 1, A and C). Thus, the generated state is actually a superposition of NOON states with various photon numbers, each of which contributes to the enhanced phase sensitivity. As a result, the current method could allow exceeding of the standard quantum limit while accounting for the complete photon number distribution (*25*).

It is interesting that a setup similar to the one in Fig. 2A, but with much stronger light fields, is commonly used for obtaining quantum noise reduction via homodyne detection (*6*). Homodyne detection is a highly developed technique based on the measurement of the continuous-variable field quadratures. Our experiment shows that extending the concept of squeezed vacuum and coherent light interference into the weak local oscillator regime is extremely fruitful. The states emerging from this interference, for a given N, are almost perfect NOON states. This implies a fundamental connection between quantum noise reduction (with continuous variables) and creation of NOON states (in photon number–resolving experiments).

The key to extending this work to even higher NOON states is in improving the overall transmission. This highlights the need for high-purity SPDC sources that can be spectrally mode-matched to coherent states (*28*–*30*). Improved single-mode coupling of the photon pairs and high-efficiency photon number–resolving detectors (*31*, *32*) would also be extremely beneficial. The inherent scalability opens the way to exciting applications in high-sensitivity interferometry, quantum imaging, and sub-Rayleigh lithography.

References and Notes

1. M. Nielsen, I. Chuang, *Quantum Computation and Quantum Information* (Cambridge Univ. Press, Cambridge, 2000).
2. J. Dowling, *Contemp. Phys.* **49**, 125 (2008).
3. E. Schrödinger, *Naturwissenschaften* **23**, 807 (1935).
4. L. Aolita, R. Chaves, D. Cavalcanti, A. Acín, L. Davidovich, *Phys. Rev. Lett.* **100**, 080501 (2008).
5. H. S. Eisenberg, G. Khoury, G. A. Durkin, C. Simon, D. Bouwmeester, *Phys. Rev. Lett.* **93**, 193901 (2004).
6. C. C. Gerry, P. L. Knight, *Introductory Quantum Optics* (Cambridge Univ. Press, Cambridge, 2005).
7. A. N. Boto *et al.*, *Phys. Rev. Lett.* **85**, 2733 (2000).
8. J. A. Jones *et al.*, *Science* **324**, 1166 (2009).
9. Y.-A. Chen *et al.*, *Phys. Rev. Lett.* **104**, 043601 (2010).
10. K. T. McCusker, P. G. Kwiat, *Phys. Rev. Lett.* **103**, 163602 (2009).
11. K. T. Kapale, J. P. Dowling, *Phys. Rev. Lett.* **99**, 053602 (2007).
12. H. Cable, J. P. Dowling, *Phys. Rev. Lett.* **99**, 163604 (2007).
13. G. J. Pryde, A. G. White, *Phys. Rev. A* **68**, 052315 (2003).
14. J. Fiurášek, *Phys. Rev. A* **65**, 053818 (2002).
15. H. F. Hofmann, *Phys. Rev. A* **70**, 023812 (2004).
16. M. D'Angelo, M. V. Chekhova, Y. Shih, *Phys. Rev. Lett.* **87**, 013602 (2001).
17. M. W. Mitchell, J. S. Lundeen, A. M. Steinberg, *Nature* **429**, 161 (2004).
18. H. Kim, H. S. Park, S.-K. Choi, *Opt. Express* **17**, 19720 (2009).
19. P. Walther *et al.*, *Nature* **429**, 158 (2004).
20. B. H. Liu *et al.*, *Phys. Rev. A* **77**, 023815 (2008).
21. K. J. Resch *et al.*, *Phys. Rev. Lett.* **98**, 223601 (2007).
22. R. Okamoto *et al.*, *N. J. Phys.* **10**, 073033 (2008).
23. T. Nagata, R. Okamoto, J. L. O'Brien, K. Sasaki, S. Takeuchi, *Science* **316**, 726 (2007).
24. H. F. Hofmann, T. Ono, *Phys. Rev. A* **76**, 031806 (2007).
25. L. Pezzé, A. Smerzi, *Phys. Rev. Lett.* **100**, 073601 (2008).
26. See supporting material on *Science* Online.
27. I. Afek, O. Ambar, Y. Silberberg, *Phys. Rev. Lett.* **104**, 123602 (2010).
28. P. J. Mosley *et al.*, *Phys. Rev. Lett.* **100**, 133601 (2008).
29. P. J. Mosley, J. S. Lundeen, B. J. Smith, I. A. Walmsley, *N. J. Phys.* **10**, 093011 (2008).
30. A. Valencia, A. Ceré, X. Shi, G. Molina-Terriza, J. P. Torres, *Phys. Rev. Lett.* **99**, 243601 (2007).
31. C. Silberhorn, *Contemp. Phys.* **48**, 143 (2007).
32. A. E. Lita, A. J. Miller, S. W. Nam, *Opt. Express* **16**, 3032 (2008).

33. We thank B. Dayan for helpful discussions. Supported by an Ilan Ramon Fellowship (I.A.) and the German-Israeli Foundation for Scientific Research and Development.

Supporting Online Material

www.sciencemag.org/cgi/content/full/328/5980/879/DC1
SOM Text
Fig. S1
References

10 February 2010; accepted 13 April 2010
10.1126/science.1188172

High-NOON States by Mixing Quantum and Classical Light
Itai Afek, Oron Ambar and Yaron Silberberg (May 13, 2010)
Science **328** (5980), 879-881. [doi: 10.1126/science.1188172]

Editor's Summary

All and Nothing

Entanglement, where a system can be in a superposition of a number of distinct states simultaneously, is a principle at the foundation of quantum mechanics (recall Schrödinger's cat, which is both dead and alive). It can also be used in many applications––imaging, communication, patterning, and metrology––with the effect being amplified by entangling larger systems. However, the systematic generation of "large" entangled systems is challenging. **Afek *et al.*** (p. 879; see the Perspective by **Wildfeuer**) present a technique for generating many-photon entanglement in so-called NOON states, where there are two possible paths and *N* photons in one path and 0 in the other ––the system being a superposition of "all and nothing" states. Mixing of entangled pairs with classical light at a beam splitter formed up to five photon-entangled states. The technique should be generally applicable to generate higher-order entangled states.